Quantum thermodynamic cycle with quantum phase transition

Yu-Han Ma,[1,2] Shan-He Su,[1] and Chang-Pu Sun[1,2,*]
[1]*Beijing Computational Science Research Center, Beijing 100193, China*
[2]*Graduate School of Chinese Academy of Engineering Physics, Beijing 100084, China*
(Received 26 May 2017; published 21 August 2017)

With the Lipkin-Meshkov-Glick (LMG) model as an illustration, we construct a thermodynamic cycle composed of two isothermal processes and two isomagnetic field processes, and we study the thermodynamic performance of this cycle accompanied by the quantum phase transition (QPT). We find that for a finite particle system working below the critical temperature, the efficiency of the cycle is capable of approaching the Carnot limit when the external magnetic field λ_1 corresponding to one of the isomagnetic processes reaches the cross point of the ground states' energy level, which can become the critical point of the QPT in the large-N limit. Our analysis proves that the system's energy level crossings at low-temperature limits can lead to a significant improvement in the efficiency of the quantum heat engine. In the case of the thermodynamics limit ($N\to\infty$), the analytical partition function is obtained to study the efficiency of the cycle at high- and low-temperature limits. At low temperatures, when the magnetic fields of the isothermal processes are located on both sides of the critical point of the QPT, the cycle reaches maximum efficiency, and the Carnot efficiency can be achieved. This observation demonstrates that the QPT of the LMG model below critical temperature is beneficial to the thermodynamic cycle's operation.

DOI: 10.1103/PhysRevE.96.022143

I. INTRODUCTION

A heat engine is a machine that allows the working substance to draw heat from a heat bath through a thermodynamic cycle and to use part of the extracted energy to do work. Carnot's theorem states that a reversible heat engine operating between two heat baths has a maximum efficiency, which is known as the Carnot efficiency, and it serves as an upper bound on the efficiency of any irreversible heat engines running between the same heat baths. In recent years, focus has been given to circumstances in which working substances exhibit quantum behaviors. Heat engines that adopt the quantum system as the working substance are called quantum heat engines [1–5]. When examining these engines, a connection can be made between the definitions of heat and work and the microscopic states of the working substances [6–8]. As a result, we can calculate the efficiency of a thermodynamic cycle from a more fundamental perspective. Different working substances, such as harmonic oscillators [9–11], spin systems [12,13], and multilevel atoms [7,14,15], have been studied to construct quantum heat engines. The basic motivation for designing quantum heat engines is to use the quantum properties of working substances or heat baths to improve the engines' efficiencies [16,17].

If the working substances consist of quantum particles with interaction, the quantum phase transition (QPT) may occur below the critical temperature due to the continuous tuning of a specific external parameter. The ground state of the system will vary enormously due to the QPT [18,19]. An interesting question that arises here is whether the QPT of the working substance can improve the efficiency of the quantum heat engine. This question inspired us to construct a quantum heat engine by taking advantage of the QPT effect in the Lipkin-Meshkov-Glick (LMG) model [20–23]. The LMG model has been studied in different experimental systems, such as platforms with Bose-Einstein condensates [24–27] and with trapped ions [28,29]. We will prove that when the QPT of the LMG model takes place below the critical temperature, the efficiency of the quantum heat engine is improved and will achieve the Carnot efficiency.

This paper is organized as follows: In Sec. II, we diagonalize the Hamiltonian of the LMG model and analyze its energy spectra with level crossing. In Sec. III, the entropy of the LMG model in the thermal equilibrium state is calculated. The thermodynamic cycle constructed by the LMG model and the efficiency expression of this cycle are given in Sec. IV. In Sec. V, we carefully analyze the efficiency of the heat engine with a finite number of particles, and we give the efficiency of the heat engine at the cross points of the ground states' energy level. In Sec. VI, we calculate the analytical expression of the efficiency of the cycle in different cases when the particle number is taking the thermodynamic limit. Conclusions are given in Sec. VII

II. LIPKIN-MESHKOV-GLICK MODEL

A. Diagonalization of the Hamiltonian

We suppose that the working substance of the quantum heat engine is a spin system with interaction, which can be described by the Lipkin-Meshkov-Glick (LMG) model [20–22]. Let $J_\alpha = \frac{1}{2}\sum_{i=1}^{N}\sigma_\alpha^i$ be the total spin of the system, where $\sigma_i^\alpha(\alpha\in\{x,y,z\})$ are the Pauli operators of the ith spin. The Hamiltonian of the LMG model reads

$$H = \varepsilon J_z + V\left(J_x^2 - J_y^2\right) + W\left(J^2 - J_z^2\right), \tag{1}$$

where $J^2 = \sum_{\alpha=x,y,z} J_\alpha^2$, V and W are the parameters describing the interaction strengths between spins, and ε is the intensity of the external magnetic field. Now, by defining $\lambda = -\varepsilon/2$, $\lambda_0/N = -(W+V)/2$, and setting $\gamma = (W-V)/(W+V) = 1$ [22,23,30], we can simplify the

*cpsun@csrc.ac.cn

 ©2017 American Physical Society

Hamiltonian as

$$H = -\frac{2\lambda_0}{N}\left(J^2 - J_z^2\right) - 2\lambda J_z. \tag{2}$$

The ground state of H lies in the subspace spanned by $\{|N/2,M\rangle, M \in [-N/2, N/2]\}$. M is restricted to an integer for even N. For odd N, M is a half-integer between $-N/2$ and $N/2$. The state $|N/2,M\rangle$ satisfies

$$J_z\left|\frac{N}{2},M\right\rangle = M\left|\frac{N}{2},M\right\rangle \tag{3}$$

and

$$J^2\left|\frac{N}{2},M\right\rangle = \frac{N}{2}\left(\frac{N}{2}+1\right)\left|\frac{N}{2},M\right\rangle. \tag{4}$$

By taking $\lambda_0 = 1$, the eigenenergy corresponding to $|N/2,M\rangle$ is explicitly obtained as

$$E(M) = \frac{2}{N}\left(M - \frac{N\lambda}{2}\right)^2 - \frac{N}{2}(1+\lambda^2) - 1. \tag{5}$$

Obviously, the minimum value of $E(M)$ is at $M = N\lambda/2$, so that the ground state of the LMG model is λ-dependent, i.e.,

$$|G\rangle = \begin{cases} \left|\frac{N}{2},\frac{N}{2}\right\rangle & (\lambda > 1), \\ \left|\frac{N}{2},I(\lambda)\right\rangle & (0 < \lambda < 1). \end{cases} \tag{6}$$

$I(\lambda)$ is the integer or half-integer nearest to $N\lambda/2$. Equation (6) indicates that the quantum phase transition (QPT) arises at the critical point $\lambda_c = 1$ [23].

B. Energy level crossing of the ground states

It follows from Eq. (6) that the ground state of the LMG model is $|N/2,I(\lambda)\rangle$ for $0 < \lambda < 1$ if $N\lambda/2 = k + \frac{1}{2}$ is a half-integer for $k = 0,1,2,\ldots$. Equation (5) indicates that the states $|N/2,M = k\rangle$ and $|N/2,M = k+1\rangle$ have the same eigenenergy, and both of them are ground states. Therefore, when $\lambda(k) = (2k+1)/N$, the ground state is degenerate. Because the energy level crossing of the ground states only appears when $\lambda < 1$, the integer $k \leqslant (N-2)/2$. For even N, the number of cross points equals $N/2$. The last cross point of the ground state is at $\lambda(k = N/2-1) = 1 - 1/N$. In the thermodynamic limit ($N \to \infty$),

$$\lim_{N\to\infty} \lambda(k = N/2-1) = 1 = \lambda_c, \tag{7}$$

which means that the last cross point of the energy levels of the ground states is exactly the critical point for the QPT.

III. ENTROPY OF THE WORKING SUBSTANCE

To calculate the heat exchange in the isothermal processes of a thermodynamic cycle, we need to discuss the entropy of the working substance. Considering the LMG model in thermal contact with a heat bath with temperature T_0, the density matrix operator in the canonical ensemble can be written as

$$\rho = \frac{1}{Z}\sum_{M=-N/2}^{N/2} e^{-\beta_0 E(M)}\left|\frac{N}{2},M\right\rangle\left\langle\frac{N}{2},M\right|. \tag{8}$$

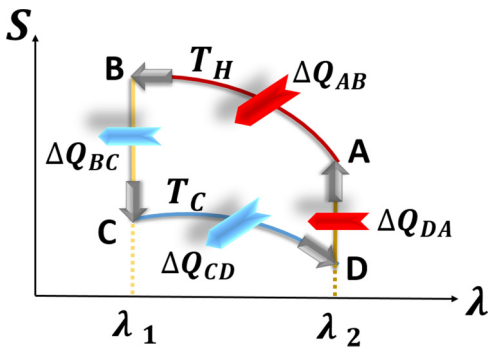

FIG. 1. Entropy-magnetic diagram ($S-\lambda$) of the thermodynamic cycle based on the LMG model. Here, λ_1 and λ_2 are the magnetic fields in the two isomagnetic field processes from B to C and from D to A. T_H and T_C are the temperatures of the two heat baths.

Here, $Z = \sum_M \exp[-\beta_0 E(M)]$ is the partition function and $\beta_0 = 1/T_0$ is the inverse temperature, as we take the Boltzmann constant $k_B = 1$. By using Eq. (8), the entropy of the working substance is obtained as

$$S = -\mathrm{Tr}(\rho \ln \rho) = -\sum_{M=-N/2}^{N/2} \frac{e^{-\beta_0 E(M)}}{Z} \ln \frac{e^{-\beta_0 E(M)}}{Z}. \tag{9}$$

According to Eq. (5), when $\lambda(k) = (2k+1)/N$, the states $|N/2,M = k\rangle$ and $|N/2,M = k+1\rangle$ have the same energy and are degenerate. This implies that the entropy of the system at $T = 0$ has a sudden abrupt rise at the energy level crossing.

IV. QUANTUM HEAT ENGINE BASED ON THE LMG MODEL

In this section, we build a quantum heat engine with a spin system, which is modeled as the LMG model. In the thermodynamic cycle (Fig. 1), the processes from A to B and from C to D are quantum isothermal processes, while the processes from B to C and from D to A are isomagnetic field processes.

During the isothermal process from A to B (C to D), the system is kept in contact with a heat bath at temperature T_H (T_C). The external magnetic field, which is regarded as the generalized coordinate in this thermodynamic cycle, is slowly reduced (increased) from λ_2 (λ_1) to λ_1 (λ_2). ΔQ_{AB} and ΔQ_{CD} represent the amounts of heat exchange between the system and the heat baths during the two isothermal processes, respectively. The working substance is always kept in thermal equilibrium with the heat bath by assuming that the energy levels of the system change much more slowly than the relaxation rates.

At the beginning of the isomagnetic field process from B to C (D to A), the system is rapidly brought into thermal contact with the heat bath at low temperature T_C (high temperature T_H). No work has been done during this process, because the external magnetic field is fixed at λ_1 (λ_2) and the eigenenergies of the working substance remain unchanged [3]. The amount of heat exchange between the system and the heat baths ΔQ_{BC} (ΔQ_{DA}) is equal to the change in the internal energy of the system.

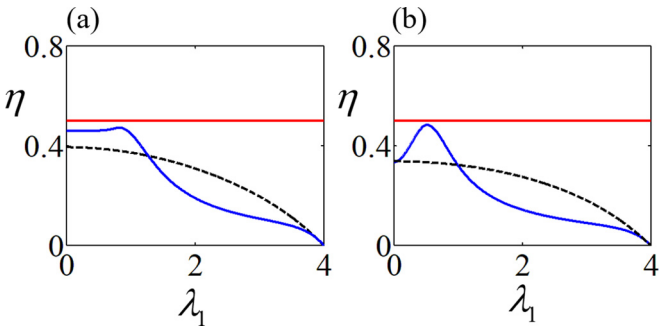

FIG. 2. Diagrams of the efficiency η as a function of λ_1 for the system with $N = 20$ in (a) and $N = 2$ in (b). The blue solid line and the black dotted line correspond to the high-temperature heat bath at $T_H = 0.8$ and 80, respectively. Here we guarantee that the Carnot efficiency of each curve equals 0.5, as indicated by the red solid line.

Based on the definition of the entropy and the first law of thermodynamics, we can calculate the amount of heat exchange in each thermodynamic process as

$$\Delta Q_{AB} = T_H(S_B - S_A), \tag{10a}$$
$$\Delta Q_{BC} = U_C - U_B, \tag{10b}$$
$$\Delta Q_{CD} = T_C(S_D - S_C), \tag{10c}$$
$$\Delta Q_{DA} = U_A - U_D. \tag{10d}$$

Here, S_α is the entropy of the system in A, B, C, and D points in the cycle. The system's internal energy $U_\alpha = \sum_i p_i(\lambda_\alpha, T_\alpha)E_i(\lambda_\alpha)$ [7]. As a result, the efficiency of the thermodynamic cycle is

$$\eta = \frac{W}{Q_H} = \frac{\Delta Q_{AB} + \Delta Q_{BC} + \Delta Q_{CD} + \Delta Q_{DA}}{\Delta Q_{AB} + \Delta Q_{DA}}, \tag{11}$$

where the work output per cycle is $W = \Delta Q_{AB} + \Delta Q_{BC} + \Delta Q_{CD} + \Delta Q_{DA}$. From Eq. (11) and Fig. 1, one can find that the net amount of heat input Q_H into the thermodynamic cycle is determined by the heat transfer ΔQ_{AB} between the system and the heat bath at temperature T_H during the isothermal process from A to B and that of the heat transfer ΔQ_{DA} in the isomagnetic field process from D to A. For $N = 2$ (or 20), $T_H = 0.8$ (or 80), and $\eta_C = (T_H - T_C)/T_H = 0.5$, we can numerically calculate the efficiency of this heat engine from Eqs. (5), (9), and (11) with $\lambda_2 = 4$ and $\lambda_1 \in [0,4]$. The results are shown in Figs. 2(a) and 2(b). It is found in Fig. 2(a) that if T_H and T_C are both very low, the efficiency of the cycle is capable of approaching the Carnot efficiency when λ_1 is below the QPT point of the LMG model. In Fig. 2(b), we notice that when $N = 2$, there is a maximum value of efficiency at $\lambda_1 \approx 0.5$. According to Sec. II B, the cross point of the ground states' energy levels is just located at $\lambda_1 = 1/2$. In the next section, we will prove theoretically and numerically that the position of the maximum efficiency of the quantum heat engine is always close to the energy level cross points.

V. MAXIMUM EFFICIENCY OF THE HEAT ENGINE FOR A SYSTEM WITH FINITE N

A. System with $N = 2$

The eigenenergies for the LMG model with two interacting spins are $E_{-1} = 2\lambda - 1$, $E_0 = -2$, and $E_1 = -2\lambda - 1$. The cross point of the ground state's energy levels is at $\lambda_1 = 1/2$. When $\beta \gg 1$ and $\lambda_2 \gg 1$, the population of the system in the ground state is

$$p(\lambda_2,\beta) = \frac{e^{2\beta\lambda_2}}{e^{2\beta\lambda_2} + e^{-2\beta\lambda_2} + e^{\beta}} \approx 1,$$

which means that the system is mostly in its ground state. As a result, $S_A = S(\lambda_2,\beta_H) \approx 0$ and $S_D = S(\lambda_2,\beta_C) \approx 0 (\beta_C > \beta_H \gg 1)$. Therefore, the heat transfer ΔQ_{DA} in the isomagnetic process from D to A is written as

$$\Delta Q_{DA} = U_A - U_D = E_G^{\lambda_2} - E_G^{\lambda_2} = 0. \tag{12}$$

In this case, the efficiency of the thermodynamic cycle is

$$\eta = \frac{T_H S_B + U_C - U_B - T_C S_C}{T_H S_B}. \tag{13}$$

Notice that $S(\lambda_\alpha,\beta_\alpha) = U_\alpha/T_\alpha + \ln Z_\alpha$. The expression of the work can be simplified as $W = T_H \ln Z_B - T_C \ln Z_C$, where the partition function is

$$Z(\lambda,\beta) = e^{\beta}[e^{-2\beta\lambda} + e^{2\beta\lambda} + e^{\beta}]. \tag{14}$$

When $\beta_C > \beta_H \gg 1$ and $e^{-2\beta\lambda_1} \ll 1 (\lambda_1 \neq 0)$, the partition functions at points B and C of the thermodynamic cycle are

$$Z_B \approx e^{2\beta_H(2\lambda_1+1)}[1 + e^{\beta_H(1-2\lambda_1)}] \tag{15}$$

and

$$Z_C \approx e^{2\beta_C(2\lambda_1+1)}[1 + e^{\beta_C(1-2\lambda_1)}], \tag{16}$$

respectively. Combining Eqs. (15) and (16), we see that

$$W = \frac{\ln[1 + e^{\beta_H(1-2\lambda_1)}]}{\beta_H} - \frac{\ln[1 + e^{\beta_C(1-2\lambda_1)}]}{\beta_C}.$$

Differentiating W with respect to λ_1, one can write

$$\frac{\partial W}{\partial \lambda_1} = 2\frac{e^{\beta_C(1-2\lambda_1)} - e^{\beta_H(1-2\lambda_1)}}{[1 + e^{\beta_H(1-2\lambda_1)}][1 + e^{\beta_C(1-2\lambda_1)}]}. \tag{17}$$

As $\beta_C > \beta_H$, it is found that

$$\frac{\partial W}{\partial \lambda_1} > 0 \quad \left(\lambda_1 < \frac{1}{2}\right),$$
$$\frac{\partial W}{\partial \lambda_1} = 0 \quad \left(\lambda_1 = \frac{1}{2}\right),$$
$$\frac{\partial W}{\partial \lambda_1} < 0 \quad \left(\lambda_1 > \frac{1}{2}\right).$$

This means that the work W of this cycle has a maximum value at $\lambda_1 = 1/2$, which is exactly the cross point of the energy level of the ground states. Now we differentiate Q_H with respect to λ_1,

$$\frac{\partial Q_H}{\partial \lambda_1} = T_H \frac{\partial S_B}{\partial \lambda_1} = \frac{\partial U_B}{\partial \lambda_1} + T_H \frac{\partial(\ln Z_B)}{\partial \lambda_1}. \tag{18}$$

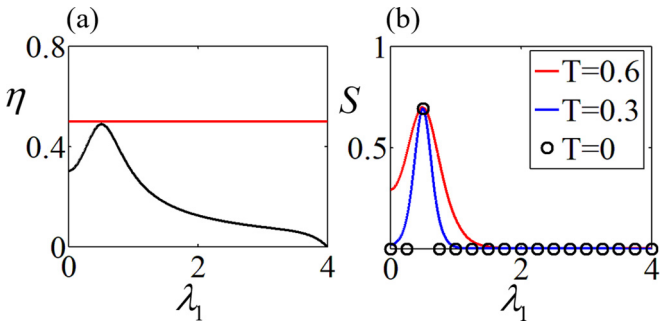

FIG. 3. (a) Diagram of the efficiency η as a function of λ_1 for the system with $N = 2$. $T_H = 0.6$ is the temperature of the hot heat bath and $T_C = 0.3$ is the temperature of the cold heat bath. The black solid line represents the efficiency of the heat engine, while the red solid line represents the corresponding Carnot efficiency. (b) Diagram of the entropy S as a function of λ_1, where the red solid line, the blue solid line, and the black circle line represent the change in the entropy when the temperatures (T) of the system are at 0.6, 0.3, and 0, respectively.

It follows from Eq. (15) that

$$U_B = -\frac{\partial(\ln Z_B)}{\partial\beta_H} = \frac{-2\lambda_1 e^{2\beta_H\lambda_1} - e^{\beta_H}}{e^{2\beta_H\lambda_1}[1 + e^{\beta_H(1-2\lambda_1)}]} - 1 \tag{19}$$

and

$$\frac{\partial Z_B}{\partial\lambda_1} = 2\beta_H e^{\beta_H(2\lambda_1+1)}. \tag{20}$$

Equation (18) can now be further simplified as

$$\frac{\partial Q_H}{\partial\lambda_1} = \frac{2\beta_H e^{2\beta_H\lambda_1}}{Z_B^2} e^{\beta_H}(1 - 2\lambda_1). \tag{21}$$

With the help of Eq. (11), one can differentiate η with respect to λ_1 as

$$\frac{\partial\eta}{\partial\lambda_1} = \frac{1}{Q_H^2}\left(\frac{\partial W}{\partial\lambda_1}Q_H - \frac{\partial Q_H}{\partial\lambda_1}W\right). \tag{22}$$

Combining Eqs. (17), (21), (22), and taking $\lambda_1 = 1/2 + \delta$ ($\delta \ll 1$), we find that

$$\left[\frac{\partial\eta}{\partial\lambda_1}\right]_{\lambda_1=\frac{1}{2}+\delta} = \frac{\beta_H^2}{\ln 2}\left(2 - \frac{T_H}{T_C} - \frac{T_C}{T_H}\right)\delta.$$

Finally, we can conclude that

$$\mathrm{sgn}\left\{\left[\frac{\partial\eta}{\partial\lambda_1}\right]_{\lambda_1=\frac{1}{2}+\delta}\right\} = -\mathrm{sgn}(\delta), \tag{23}$$

where $\mathrm{sgn}(x) \equiv x/|x|$ is the sign function. Equation (23) shows that the efficiency of such a thermodynamic cycle has a maximum value at $\lambda_1 = 1/2$ and $\eta(\lambda_1 = 1/2) = \eta_{\mathrm{Carnot}}$. This result can be checked by the numerical calculation directly, where we take $N = 2$, $T_H = 0.6$, $T_C = 0.3$, $\lambda_1 \in [0,4]$, and $\lambda_2 = 4$. The diagram of η as a function of λ_1 is plotted in Fig. 3(a), and the entropy of the system at the given temperature as a function of λ_1 is shown in Fig. 3(b). It can be found in Fig. 3(a) that the efficiency takes the maximum value at $\lambda_1 = 0.5$ and is equal to the Carnot efficiency. In Fig. 3(b), one can see that when $\lambda_1 = 0.5$, the blue line is tangent to the red line, and the corresponding entropy value is the same as the entropy of the system at zero temperature represented by the black circle. When $\lambda_1 = 1/2$, the ground states are crossing with $U_B \approx U_C = -1$, and $S_B \approx S_C \approx \ln 2$. As a result,

$$\eta = \frac{T_H S_B - T_C S_C}{T_H S_B} \approx \eta_C, \tag{24}$$

which is also observed in Fig. 3(b). From another point of view, when λ_1 is at the cross point of the ground states' energy levels, the internal energy of point B is equal to that of point C. This implies that there is no heat exchange between the system and the bath in the process from B to C. On the other hand, Eq. (12) indicates that the heat transfer in the process from D to A does not exist ($\lambda_2 \gg 1$). There is no heat transfer in the two isomagnetic processes of the thermodynamic cycle. Thus, from the entropy diagram, the thermodynamic cycle that we construct is similar to the Carnot cycle. This is the fundamental reason why the efficiency of the quantum heat engine we proposed can achieve Carnot efficiency in this particular case.

B. System with $N > 2$

For $N > 2$, the cross points are located at $\lambda_1(k) = (2k + 1)/N (k = 0,1,\ldots,N/2 - 1)$. Considering Eq. (5), we have

$$E(M = k) = E(M = k + 1) < E(M \neq k, k + 1) < 0.$$

When $\beta \gg 1$,

$$e^{-\beta E(M=k)} = e^{-\beta E(M=k+1)} \gg e^{-\beta E(M\neq k,k+1)},$$

the partition function

$$Z = \sum_M e^{-\beta E(M)} \approx 2e^{-\beta E(k)}.$$

The entropy

$$\begin{aligned} S &= \beta U(\lambda_1(k), \beta \gg 1) + \ln Z(\lambda_1(k), \beta \gg 1) \\ &\approx \beta E(k) + \ln[2e^{-\beta E(k)}] = \ln 2, \end{aligned}$$

which is independent of the temperature. As a result,

$$\eta = \frac{T_H S(\lambda_1, T_H) - T_C S(\lambda_1, T_C)}{T_H S(\lambda_1, T_H)} \approx \eta_C. \tag{25}$$

This implies that when the temperatures of the two heat baths are very low and λ_1 takes the values for reaching the cross point of the ground states' energy levels, the efficiency of the heat engine approaches Carnot efficiency. The numerical results of the efficiency of the thermodynamic cycle with $N = 4$, 6, 8, and 10 are given in Fig. 4. One can easily check that under different conditions, there are $N/2$ peaks in the diagram of η varying λ_1, which is exactly the same as the number of cross points of the ground states' energy level. The efficiency values corresponding to these peaks are also consistent with the prediction in Eq. (25), which is close to the Carnot efficiency η_C. These figures validate our heretical analysis that the maximum value of the cycle's efficiency is always obtained when λ_1 is at the cross points of energy levels. It is clear in these figures that there are $N/2$ peaks in the curve of efficiency for the N-spin system. As N increases, the peaks gradually become flat and approach the red straight

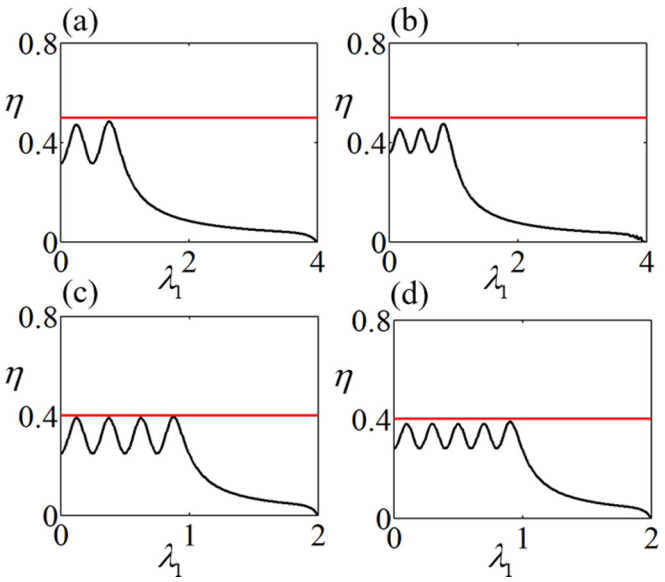

FIG. 4. Diagrams of the efficiency η as a function of λ_1, where the black solid lines represent the efficiency of the heat engine while the red solid lines represent the corresponding Carnot efficiency. (a) For the system with $N = 4$, the parameters $T_H = 0.3$, $T_C = 0.15$, $\lambda_1 \in [0,4]$, and $\lambda_2 = 4$. (b) For the system with $N = 6$, the parameters $T_H = 0.2$, $T_C = 0.1$, $\lambda_1 \in [0,4]$, and $\lambda_2 = 4$. (c) For the system with $N = 8$, the parameters $T_H = 0.1$, $T_C = 0.06$, $\lambda_1 \in [0,2]$, and $\lambda_2 = 2$. (d) For the system with $N = 10$, the parameters $T_H = 0.1$, $T_C = 0.06$, $\lambda_1 \in [0,2]$, and $\lambda_2 = 2$.

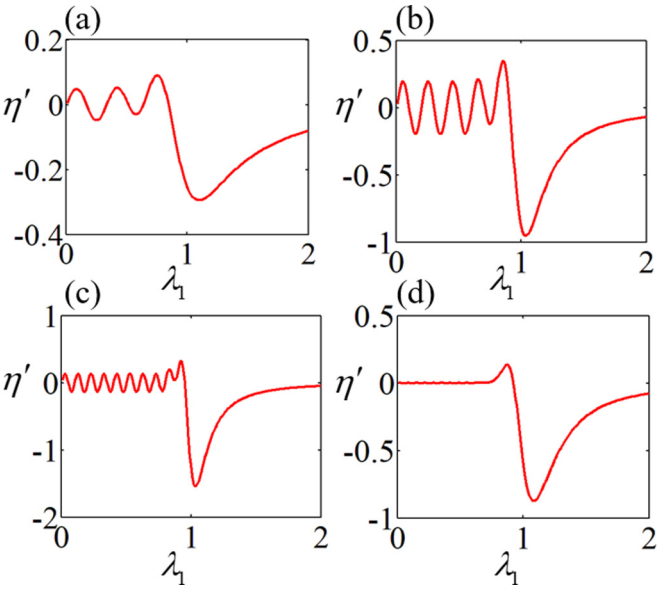

FIG. 5. Diagrams of $\eta' = \partial\eta/(\partial\lambda_1)$ as a function of λ_1, where $\lambda_1 \in [0,2]$ and $\lambda_2 = 2$. (a) For the system with $N = 6$, the parameters $T_H = 0.3$ and $T_C = 0.2$. (b) For the system with $N = 10$, the parameters $T_H = 0.2$ and $T_C = 0.1$. (c) For the system with $N = 20$, the parameters $T_H = 0.12$ and $T_C = 0.06$. (d) For the system with $N = 30$, the parameters $T_H = 0.2$ and $T_C = 0.1$.

line marked by the Carnot efficiency. As shown in Sec. II B, the number of cross points of the ground states increases as N increases. Thus, we can reasonably speculate that the efficiency of the thermodynamic cycle at the low-temperature limit will always approach the Carnot efficiency when $\lambda_1 < \lambda_c$, and N is taken to be the thermodynamic limit ($N \to \infty$). This will be proven analytically in the next section. To further demonstrate the relationship between the cycle's efficiency and the cross points of the energy levels, the plot of $\eta' = \partial\eta/\partial\lambda_1$ as a function of λ_1 under different situations is calculated and illuminated in Fig. 5. The diagrams show that there is a valley around $\lambda_c = 1$. When N is small, there are some fluctuations in the curves, which correspond exactly to the cross points of the ground states' energy levels. With the increase of N, the cross points of the ground states' energy level of the system become more dense, and the fluctuations diminish until they disappear.

VI. EFFICIENCY OF THE HEAT ENGINE UNDER THE THERMODYNAMIC LIMIT $N \to \infty$

When N is taken to be the thermodynamic limit ($N \to \infty$), the partition function can be approximated as (for details, see the Appendix)

$$Z = \frac{e^{\beta N(1+\lambda^2)/2}}{\sqrt{2N\beta}}\left[\mathrm{erf}\left(\frac{a+1}{K}\right) + \mathrm{erf}\left(\frac{-a}{K}\right)\right], \tag{26}$$

where $\mathrm{erf}(x) = \sqrt{4/\pi}\int_0^x \exp(-\eta^2)d\eta$ is the Gauss error function, $a = -(1+\lambda)/2$, and $K = 1/\sqrt{2N\beta}$. With the help of Eq. (26), we can discuss the efficiency of the heat engine under different circumstances.

A. Efficiency at the high-temperature limit

For $T \gg 1$, $(a+1)/K, -a/K \ll 1$,

$$\mathrm{erf}\left(\frac{a+1}{K}\right) \approx -\sqrt{\frac{2N\beta}{\pi}}(1-\lambda)$$

and

$$\mathrm{erf}\left(\frac{-a}{K}\right) \approx \sqrt{\frac{2N\beta}{\pi}}(1+\lambda).$$

We have

$$Z \approx \frac{1}{\sqrt{\pi}}\exp\left[\frac{N\beta}{2}(1+\beta\lambda^2)\right], \tag{27}$$

where the relation $\mathrm{erf}(\sqrt{2N}/2) \approx \mathrm{erf}(\infty) = 1$ has been used. Taking the logarithm of both sides of Eq. (27), we have

$$\ln Z \approx \frac{1}{2}\ln\pi + \frac{N\beta}{2}(1+\beta\lambda^2). \tag{28}$$

As a result, the internal energy

$$U = -\frac{\partial(\ln Z)}{\partial\beta} = -\left(\frac{N}{2} + N\beta\lambda^2\right). \tag{29}$$

It follows from Eqs. (11), (28), and (29) that

$$\eta = \frac{(\lambda_2^2 - \lambda_1^2)(\beta_C - \beta_H)}{(\lambda_1^2 - \lambda_2^2)\beta_H + 2\beta_C\lambda_2^2 - 2\beta_H\lambda_1^2}.$$

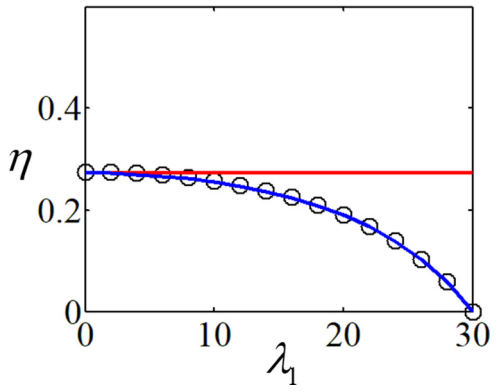

FIG. 6. Diagrams of η as a function of λ_1. Here, the black circle line denotes the numerical results, the blue solid line denotes the analytical results of Eq. (30), and the red solid line denotes $\eta_0 = \eta_C/(1+\eta_C)$, where η_C is the corresponding Carnot efficiency. The temperatures of the two heat baths are $T_H = 800$ and $T_C = 500$, respectively.

By introducing $\kappa \equiv \lambda_1/\lambda_2 \in [0,1]$, the efficiency can be further simplified as

$$\eta = \frac{(1-\kappa^2)\eta_C}{1-\kappa^2+\eta_C(1+\kappa^2)}, \tag{30}$$

which is independent of N. In particular, when $\kappa \ll 1$, $\eta_0 = \eta_C/(1+\eta_C)$. For purposes of verifying the above analysis, we give the numerical result of the efficiency as a function of λ_1 with $N = 100$, $\lambda_1 \in [0,30]$, and $\lambda_2 = 30$, as shown in Fig. 6. It can be seen in Fig. 6 that Eq. (30) is consistent with the numerical result, and when $\lambda_1 \ll \lambda_2$, the efficiency approaches $\eta_0 = \eta_C/(1+\eta_C)$.

B. Efficiency at the low-temperature limit

In this section, we consider the working substance coming into contact with the baths having a temperature $T \ll 1$. In the following, we will discuss the partition function in two cases involving $\lambda < 1$ and $\lambda > 1$. If $\lambda < 1$,

$$\mathrm{erf}\left(\frac{a+1}{K}\right) + \mathrm{erf}\left(\frac{-a}{K}\right) \approx 2\mathrm{erf}\left(\frac{\sqrt{2N\beta}}{2}\right) = 2,$$

such that the partition function is approximated as

$$Z = \frac{2}{\sqrt{2N\beta}} \exp\left[\frac{\beta N}{2}\left(1+\lambda^2\right)\right]. \tag{31}$$

The logarithm of Eq. (31) can be written as

$$\ln Z = \ln 2 - \frac{1}{2}\ln(2N\beta) + \frac{N\beta}{2}(1+\lambda^2) \approx \frac{N\beta}{2}(1+\lambda^2). \tag{32}$$

As a result,

$$U = -\frac{\partial(\ln Z)}{\partial\beta} = -\frac{N}{2}(1+\lambda^2). \tag{33}$$

For $\lambda_1 < \lambda_2 < 1$, it follows from Eqs. (11), (32), and (33) that $\eta \approx 0$. This is checked by numerical calculation, and the results are illustrated in Figs. 7(a) and 7(b). On the other hand,

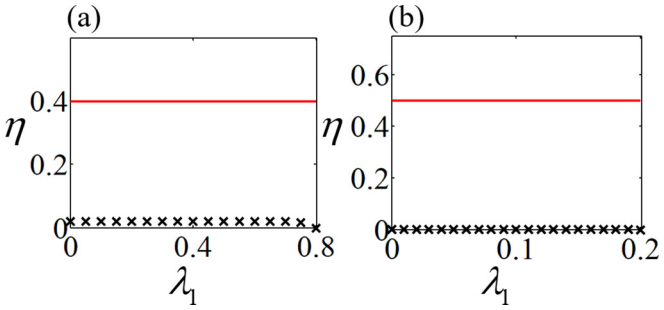

FIG. 7. Diagrams of the efficiency η as a function of λ_1, where the black crosses are the numerical results and the red solid lines represent the corresponding Carnot efficiency. (a) For the system with $N = 30$, the parameters $T_H = 0.5$, $T_C = 0.3$, $\lambda_1 \in [0,0.8]$, and $\lambda_2 = 0.8$. (b) For the system with $N = 50$, the parameters $T_H = 0.2$, $T_C = 0.1$, $\lambda_1 \in [0,0.2]$, and $\lambda_2 = 0.2$.

when $\lambda \gg 1$, one can write the energy spacing of the LMG model's eigenenergies as

$$\Delta E(M) = \left(\frac{4M}{N} - 2\lambda\right)\Delta M = \left(\frac{4M}{N} - 2\lambda\right),$$

which is approximately equal to 2λ. In this case, the system would only stay in its ground state $|N/2, N/2\rangle$. The reason is that the system cannot be excited by the thermal energy for $T \ll 1$. The partition function is now given by $Z = \exp[-\beta E(N/2)] = \exp(\beta N\lambda)$. Taking the logarithm of both sides, we have

$$\ln Z = \beta N\lambda, \tag{34}$$

and the internal energy of the system is

$$U = -\frac{\partial(\ln Z)}{\partial\beta} = -N\lambda. \tag{35}$$

Combining Eqs. (11), (32)–(35), and the condition $\lambda_1 < 1 \ll \lambda_2$, the efficiency of the thermodynamic cycle at the low-temperature limit is obtained as $\eta = \eta_C$. This indicates that the efficiency of the thermodynamic cycle is exactly the

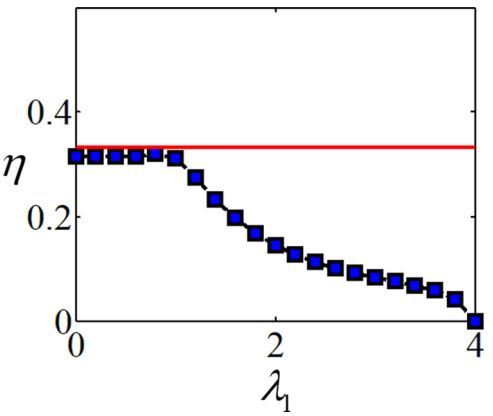

FIG. 8. Diagram of η as a function of λ_1 for the system with $N = 20$, where $\lambda_1 \in [0,4]$ and $\lambda_2 = 4$. $T_H = 0.3$ is the temperature of the hot heat bath. $T_C = 0.2$ is the temperature of the cold heat bath. Here, the blue square points are the numerical results and the red solid line is the corresponding Carnot efficiency.

Carnot efficiency for a system with $N \gg 1$. On the other hand, for $1 \ll \lambda_1 < \lambda_2$ and with the help of Eqs. (34) and (35), one has $\ln Z_B = N\beta_H\lambda_1$, $\ln Z_A = N\beta_H\lambda_2$, $\ln Z_D = N\beta_C\lambda_2$, and $\ln Z_C = N\beta_C\lambda_1$. The work and the efficiency are both equal to zero. We illustrate the numerical result in Fig. 8 to verify the above discussion, where the parameters we take are $N = 20$, $\lambda_1 \in [0,4]$, and $\lambda_2 = 4$. It can be found in Fig. 8 that the numerical results are consistent with the theoretical analysis. When $\lambda_1 < 1$, the efficiency of the heat engine is close to Carnot efficiency. When $\lambda_1 > 1$, the efficiency is rapidly reduced to zero.

VII. CONCLUSION

In summary, we have studied quantum thermodynamic cycles with a working substance modeled as the Lipkin-Meshkov-Glick (LMG) model. It is found that, for a finite system with a thermodynamic limit, the efficiency of the thermodynamic cycle can reach the Carnot limit at low temperature when the external magnetic field λ_1 corresponding to one of the isomagnetic processes reaches the cross points of the ground states' energy level. In the case of the thermodynamic limit ($N \to \infty$), the analytical partition function of the LMG model in the thermal equilibrium state is obtained and then used to calculate the efficiencies of the heat engine at the high- and low-temperature limits. We show that the quantum heat engine will achieve Carnot efficiency at low temperature, when the phases of the system in the two isomagnetic processes are different. This observation implies that the quantum phase transition (QPT) can improve the efficiency of the thermodynamic cycle. In view of the fact that the LMG model has been implemented on different experimental platforms, we expect future quantum heat engines with the QPT to have Carnot efficiency, thereby achieving the purpose of using quantum techniques to enhance device efficiency.

ACKNOWLEDGMENTS

This study is supported by the National Basic Research Program of China (Grants No. 2014CB921403 and No. 2016YFA0301201), the NSFC (Grants No. 11421063 and No. 11534002), and the NSAF (Grant No. U1530401).

APPENDIX: PARTITION FUNCTION

The partition function is given by

$$Z = \sum_{M=-N/2}^{N/2} \exp\left[-\beta\left(\frac{2M^2}{N} - 2\lambda M - \frac{N}{2} - 1\right)\right]. \quad \text{(A1)}$$

For a system under a thermodynamic limit $N \to \infty$, by taking $x \equiv M/N$, the summation in Eq. (A1) is approximated as an integral $\sum_{M=-N/2}^{M=N/2} = N\int_{-1/2}^{1/2} dx$. The partition function can be rewritten as $Z = \exp(\beta N/2)\int_{-1/2}^{1/2} \exp[-2N\beta(x^2 - \lambda x)]dx$. After some algebraic manipulation, one has

$$Z \approx \exp\left[\frac{N\beta}{2}(1+\lambda^2)\right]\int_{-1/2}^{1/2} e^{-2N\beta(x-\frac{\lambda}{2})^2} dx \quad \text{(A2)}$$

$$= \exp\left[\frac{N\beta}{2}(1+\lambda^2)\right] K \int_{a/K}^{(a+1)/K} e^{-y^2} dy. \quad \text{(A3)}$$

Here, $a \equiv -(1+\lambda)/2$ and $K \equiv 1/\sqrt{2N\beta}$. Finally, with the help of the Gauss error function $\mathrm{erf}(x) = \sqrt{4/\pi}\int_0^x \exp(-\eta^2)d\eta$, the partition function is obtained as

$$Z = \frac{e^{\beta N(1+\lambda^2)/2}}{\sqrt{2N\beta}}\left[\mathrm{erf}\left(\frac{a+1}{K}\right) + \mathrm{erf}\left(\frac{-a}{K}\right)\right]. \quad \text{(A4)}$$

[1] S. H. Su, X. Q. Luo, J. C. Chen *et al.*, Europhys. Lett. **115**, 30002 (2016).
[2] B. Lin and J. Chen, Phys. Rev. E **67**, 046105 (2003).
[3] X. L. Huang, T. Wang, and X. X. Yi, Phys. Rev. E **86**, 051105 (2012).
[4] B. H. Lin and J. C. Chen, Open Syst. Inf. Dyn. **11**, 87 (2004).
[5] F. Wu, J. He, Y. Ma, and J. Wang, Phys. Rev. E **90**, 062134 (2014).
[6] H. T. Quan, P. Zhang, and C. P. Sun, Phys. Rev. E **72**, 056110 (2005).
[7] H. T. Quan, Y. X. Liu, C. P. Sun, and F. Nori, Phys. Rev. E **76**, 031105 (2007).
[8] H. T. Quan, Phys. Rev. E **79**, 041129 (2009).
[9] Y. Rezek and R. Koslo, New J. Phys. **8**, 83 (2006).
[10] J. Rossnagel, O. Abah, F. Schmidt-Kaler, K. Singer, and E. Lutz, Phys. Rev. Lett. **112**, 030602 (2014).
[11] G. S. Agarwal and S. Chaturvedi, Phys. Rev. E **88**, 012130 (2013).
[12] E. A. Ivanchenko, Phys. Rev. E **92**, 032124 (2015).
[13] F. Altintas and O. E. Mustecaplioglu, Phys. Rev. E **92**, 022142 (2015).
[14] R. Uzdin and R. Koslo, Europhys. Lett. **108**, 40001 (2014).
[15] T. D. Kieu, Eur. Phys. J. D **39**, 115 (2006).
[16] S. H. Su, C. P. Sun, S. W. Li, and J. C. Chen, Phys. Rev. E **93**, 052103 (2016).
[17] M. O. Scully, M. S. Zubairy, G. S. Agarwal, and H. Walther, Science **299**, 862 (2003).
[18] S. Sachdev, *Quantum Phase Transition* (Cambridge University Press, Cambridge, 1999).
[19] H. T. Quan, Z. Song, X. F. Liu, P. Zanardi, and C. P. Sun, Phys. Rev. Lett. **96**, 140604 (2006).
[20] H. J. Lipkin, N. Meshkov, and A. J. Glick, Nucl. Phys. **62**, 188 (1965).
[21] N. Meshkov, A. J. Glick, and H. J. Lipkin, Nucl. Phys. **62**, 199 (1965).
[22] A. J. Glick, H. J. Lipkin, and N. Meshkov, Nucl. Phys. **62**, 211 (1965).
[23] H. T. Quan, Z. D. Wang, and C. P. Sun, Phys. Rev. A **76**, 012104 (2007).
[24] C. Gross, T. Zibold, E. Nicklas *et al.*, Nature (London) **464**, 1165 (2010).

[25] Y. C. Zhang, X. F. Zhou, X. Zhou, G. C. Guo, and Z. W. Zhou, Phys. Rev. Lett. **118**, 083604 (2017).
[26] M. F. Riedel, P. Bhi, Y. Li *et al.*, Nature (London) **464**, 1170 (2010).
[27] I. D. Leroux, M. H. Schleier-Smith, and V. Vuletic, Phys. Rev. Lett. **104**, 073602 (2010).
[28] T. Monz, P. Schindler, J. T. Barreiro, M. Chwalla, D. Nigg, W. A. Coish, M. Harlander, W. Hansel, M. Hennrich, and R. Blatt, Phys. Rev. Lett. **106**, 130506 (2011).
[29] J. G. Bohnet, B. C. Sawyer, J. W. Britton *et al.*, Science **352**, 1297 (2016).
[30] J. Ma and X. G. Wang, Phys. Rev. A **80**, 012318 (2009).